Exp Oncol 2019
41, 2, 112–122

Experimental ONCOLOGY

PROINFLAMMATORY EFFECTS OF PHOTOACTIVATED METHYLENE BLUE ON RAT MODEL OF WALKER 256 CARCINOSARCOMA

*M.C. Petrellis[1], L. Frigo[2,] *, W. Ribeiro[1], E.C.P. Leal-Junior[3], F.R. Oliveira[4], D.A. Maria[5], R.Á.B. Lopes-Martins[6]*

[1]*Department of Pharmacology, Biomedical Sciences Institute, São Paulo University, São Paulo 05508-900, Brazil*

[2]*Department of Periodontology, Dental Research Division, Guarulhos University (UnG), São Paulo 07023-070, Brazil*

[3]*Nove de Julho University, Rehabilitation Program — UNINOVE, São Paulo 01504-001, Brazil*

[4]*Department of Cellular and Developmental Biology, Biomedical Sciences Institute, São Paulo University, São Paulo 05508-900, Brazil*

[5]*Biochemistry and Biophysical Laboratory, Butantan Institute, São Paulo 05599-000, Brazil*

[6]*Biophotonics and Experimental Therapeutics Laboratory, Vale do Paraiba University — UNIVAP 2911, São José do Campos 12244-000, Brazil*

***Background*. Photodynamic therapy (PDT) is an anticancer therapy that associates the photosensitizer (PS), oxygen and light to destroy cancer cells. Methylene blue (MB) is considered a second generation phenothiazine dye with excellent photochemical properties. *Aim*: To evaluate whether MB-mediated PDT can induce oxidative stress and inflammation, therefore, interfering tumor growth. *Materials and Methods*: The study was conducted on Wistar rats transplanted with Walker 256 carcinosarcoma (W256). The proinflammatory interleukins levels (IL-1β, IL-6, IL-10, TNF-α) were determined by ELISA, mRNA expression of COX-1, COX-2, iNOS and eNOS by RT-PCR, lipid peroxidation was measured by the TBARS method. Moreover, myeloperoxidase (MPO) activity in neutrophils was determined by MPO activity assay. All indices mentioned above were determined in tumor tissue. Kaplan — Meier and Gehan — Breslow — Wilcoxon tests were used for survival analysis. *Results*: We found that the treatment of W256 with 0.1% MB + 1 J/cm^2 provoked a significant increase in the interleukins levels (IL-1β, IL-6, IL-10, TNF-α), prostaglandin E_2, the mRNA expression of COX-2, iNOS, lipid peroxidation and MPO activity in tumor tissue, which were statistically different ($p < 0.05$) compared to other experimental and control groups. The results of the estimation of survival curves show a greater probability of survival in 0.1% MB + 1 J/cm^2 (total energy dose =142.8 J/cm^2) treated group. *Conclusion*: Our results suggest that treatment of W256 with 0.1% MB + 1 J/cm^2 was able to promote cytotoxic effects in tumor tissue by the generation of reactive oxygen species causing inflammation and thus interfering in the tumor growth.**

***Key Words*: photodynamic therapy, cancer, Walker carcinosarcoma 256 cells, methylene blue, photosensitizing agent, inflammation.**

INTRODUCTION

Photodynamic therapy (PDT) is considered a minimally invasive anticancer therapy that uses an association with a photosensitizer (PS), light visible in the presence of oxygen to destroy tumor cells [1–3, 16, 19]. This procedure requires the administration of a photosensitizing drug, or a pro-drug which selectively accumulates in the tumor cells, followed by irradiation of the tumor site by an appropriate wavelength capable of triggering a photochemical reaction leading to the generation of singlet oxygen ($^1O_2$) and other reactive oxygen species (ROS). This generation of $^1O_2$ and ROS obtained during photodynamic process causes damage to the sites of PS accumulation and thus leading to the death of tumor cells [1, 4–6, 15, 19]. One of the most relevant characteristics of PS is to accumulate preferentially in tumor tissue, making the use of PDT more attractive as anticancer therapy because it demonstrates better specificity and selectivity. Thence, PDT has become the subject of extensive investigations to establish a possible therapy for several types of cancer. In fact, PDT has been shown to have more advantageous aspects because it is considered a localized therapy, much cheaper and causes fewer side effects than other conventional therapies, for example, chemotherapy, radiotherapy or surgery [6–9, 20].

Mitochondria are important complex organelles that demonstrate broad structural and functional specificity, therefore being responsible for the control of several critical processes in eukaryotic cells. Currently, mitochondria play an important role in their metabolism and in the generation of ROS, since they are strongly associated with tumor progression and chemoresistance in cancer. Thus, targeting mitochondria can have potential therapeutic benefits. The clinical use of agents in PDT can be linked with the plasma membrane or membranes of intracellular organelles. The previous study has shown that mitochondria and

Submitted: September 25, 2018.

*Correspondence: E-mail: luciofrigo@uol.com.br

Abbreviations used: COX-1 – cyclooxygenase-1; *COX-2* – cyclooxygenase-2; Dcs – dendritic cells; eNOS – endothelial nitric oxide synthase; iNOS – inducible nitric oxide synthase; IL – interleukin; J – Joule; MB – methylene blue; MPO – myeloperoxidase; NO – nitric oxide; PS – photosensitizer; PDT – photodynamic therapy; PGE_2 – prostaglandin E_2; ROS – reactive oxygen species; W256 – Walker 256 carcinosarcoma.

endoplasmic reticulum localization of PSs normally lead to the apoptotic pathway. On the other hand, the necrotic pathway may be initiated when PSs are localized in the plasma membrane or lysosomes [4, 5]. Therefore, the resulting of photodamage and cytotoxic effects during the PDT process is highly dependent on determining factors to be considered such as type of PS and its subcellular location, time of PS administration, irradiation conditions, type of tumor and the level of tissue oxygenation [5].

Three main PDT mechanisms of antitumor activity mediated by ROS contribute to the reduction and destruction of tumors: (1) direct cellular damage, (2) indirect vascular shutdown and (3) activation of immune responses against tumor cells. Direct damage to cancer cells induced by the generation of $^1O_2$ and ROS can result in cell death by both pathways apoptosis and necrosis. Recent research has identified that PDT-related lethality is strongly involved in mitochondrial membrane damage. Once the transition of mitochondrial permeability occurs due to the cellular oxidative stress caused by PDT, this event leads to rupture of the membrane potential and thus releases pro-apoptotic factors, activating different caspases and finally, cell death by apoptosis. PDT also mediates a vascular effect within tumors, thus, causes vascular damage associated tumor leading to vessel constriction, vessel permeability, leukocyte adhesion, thrombosis, and hemorrhage. These events contribute thereafter to blood flow stasis and severe and persistent post-PDT tumor hypoxia and cell death. Therefore, it has been identified that the destruction of cancer cells is associated with hypoxia and the accompanying deprivation of nutrients [6, 10–12]. The effects of PDT on the immune system have been demonstrated through inflammatory reactions during photodynamic action and are considered a crucial event in the development of the antitumor immune response. The action of PDT in cancer cells shows higher generation of immune-inflammatory markers such as heat shock proteins, complement proteins, eicosanoids, chemokines, cytokines like TNF-α, IL-6, IL-1 and different transcription factors, including NF-κB and AP-1 that induces the presentation of antigens by dendritic cells (Dcs) and the recruitment and invasion of immune cells including neutrophils, macrophage, specific cytotoxic T-lymphocytes and thus contributing to the death of tumor cells. These events lead not only to tumor destruction but also to stimulate the immune system in the recognition and destruction of cancer cells in isolated sites [4, 6, 8, 13–16, 19, 20]. However, recent research has directed that the primary antitumor response production of $CD8^+$-T cells is strongly dependent on high neutrophilia, which is considered a rich pool of cytokines that are related in the recruitment and sensitization of other immune cells [8].

Methylene blue (MB) from phenothiazinium redox cycles class is considered a second generation phenothiazine dye with excellent electrocatalytic properties. It is widely used in various biomedical and therapeutic applications, including its use as a dye or stain in diagnostic procedures and for the treatment of several diseases such as methemoglobinemia, ifosfamide-induced encephalopathy and vasoplegia associated with septic shock [21–25]. Moreover, MB shows excellent photochemical properties, thus making it a potent PS for PDT. MB has a complex photodynamic mechanism, once activated it has high quantum intersystem crossing and generate high concentrations of singlet oxygen ($^1O_2$) and ROS, which are responsible for the oxidation of biomolecules, causing severe cellular damage and cytotoxicity [24, 26–28]. Actually, research has identified that cell oxidation during PDT-induced MB follows a non-linear kinetic reaction. In addition, recent investigations with MB-induced PDT have shown that the main mode of tumor extirpation is by direct death of cancer cells rather than by collapse of tumor vascularization [27]. Due to its lipophilic characteristic, MB has shown a high affinity for cell membranes and thus tends to anchor at intracellular organelles membranes especially mitochondria, inducing apoptotic cell death by mitochondrial impairment during the PDT process [24, 27–28].

Based on these findings, the objective of this work was to evaluate that MB-mediated PDT can induce oxidative stress, inflammation and therefore interfering in tumor progression.

MATERIALS AND METHODS

Reagents. A commercial kit to measure protein quantification (Bio Rad, USA), a commercial kit to measure levels of IL-1, IL-6, IL-10 and TNF-α (R & D System, USA), Trizol (Gibco BRL, USA), a commercial kit for cDNAs synthesis SuperScript (Invitrogen, USA), a commercial kit to determine the level of prostaglandin E_2 (PGE_2) EIA — Monoclonal (Cayman Chemicon, USA), potassium phosphate buffer and hydrochloric (Mallinckrodt, Mexico), trichloroacetic acid, thiobarbituric acid, o-dianisidine dihydrochloride and peroxide hydrogen (Merck, Germany). Other reagents involved in this study were purchased in Sigma Chemical Company, USA.

Animals. Female Wistar rats weighing 200 g from Central Animal Bioterrorism of Institute of Biomedical Sciences — USP were used. They were housed in plastic cages with *ad libitum* access to food and water. Light/dark cycle (lights on at 7:00 A.M., off at 7:00 P.M.) and temperature (22 °C) were kept constant. The animals were maintained and used in accordance with the guidelines of the Committee on Care and Use of Laboratory Animal Resources, National Research Council, USA. All experiments using animals of this present study were approved by the Animal Experimentation Ethics Committee of the Institute of Biomedical Sciences, University of São Paulo, Protocol Number 67 fl 73 L2-5351.

Experimental protocol of PDT. $1 \cdot 10^7$ viable tumor cells were subcutaneously inoculated in 1 ml of phosphate buffered saline (PBS:

16.5 mM phosphate, 137 mM NaCl, 2.7 mM KCl; pH = 7.4) per rat into the right flank (tumor-bearing rats). After a period of 14 days, the animals were randomized into two different treatment protocols with five and four experimental groups, respectively (n = 8 animals per group — Table 1). The animals were maintained under ketamine + xylazine anesthesia (20 and 100 mg/kg, respectively) for the accomplishment of these two treatment protocols. The first treatment was established an intra-tumor administration of 0.1 ml MB in different concentrations for each respective group in the solid tumor mass, corresponding to three treatments on alternate days. The second treatment protocol consists of an intratumor administration of saline for the control group and with 0.1 ml MB at a concentration of 0.1% according to their respective group. After one hour, the solid tumor mass was illuminated by a diode low level laser (Thera Laser — DMC®, São Carlos, Brazil). The laser unit emitted a continuous optical output of 100 mW with a wavelength of 660 nm to a spot size area of 0.028 cm^2, giving a power density of 3.57 W/cm^2. Three different energy densities were performed (1 J/cm^2, 3 J/cm^2, 6 J/cm^2) at four equidistant points according to the respective groups corresponding to three treatments on alternate days. 24 hours after the last treatment the animals were anesthetized with halothane (1 mg/ml) for the collection biopsy and then immediately euthanized with an overdose of halothane.

Table 1. Scheme of the experimental groups

Treatment groups (n = 8)	MB dose, mg/ml	Energy dose, J/cm^2	Total energy dose (4 points), J/cm^2	Energy (J)	Output power, mW	Time, sec
Control	–	–	–	–	–	–
MB 0.1%	1	–	–	–	–	–
MB 0.3%	3	–	–	–	–	–
MB 1.0%	10	–	–	–	–	–
MB 3.0%	30	–	–	–	–	–
Control	–	–	–	–	–	–
MB 0.1% + laser 1 J/cm^2	1	35.7	142.8	1	100	10
MB 0.1% + laser 3 J/cm^2	1	107.14	428.56	3	100	30
MB 0.1% + laser 6 J/cm^2	1	214.28	857.12	6	100	60

Note: Ø spot size area = 0.028 cm^2.

For the evaluation of survival, the animals treated groups (n = 5 animals per group) of the two treatment protocols were kept under observation for a period of 30 days from the first day of treatment for the follow-up of death events.

Analysis of IL-1, IL-6, IL-10 and TNF-α levels. The samples of tumor tissue were homogenized and protein quantification was measured by the method of Bradford (1976) using a commercial kit. The measurement of IL-1, IL-6, IL-10, and TNF-α in tumor tissue samples was determined by enzyme-linked immunosorbent assay (ELISA), according to the manufacturer's manual. A spectrophotometer Spectramax plus 384 (Sunnyvale, USA) at 450–570 nm wavelength was used for reading of results.

The mRNA expression analysis of cyclooxygenase-1 (COX-1), cyclooxygenase-2 (COX-2), inducible (iNOS) and endothelial nitric oxide synthase (eNOS) by RT-PCR. The mRNA expression of COX-1, COX-2, iNOS, and eNOS were determined by quantitative RT-PCR. The total RNA from samples was extracted using Trizol. The isolated RNA was dissolved in DEPC-treated water and quantified by spectrophotometry at 260 nm wavelength, checking the ratio of 260/280 nm wavelength. The integrity of the RNA was verified by electrophoresis on agarose gel containing ethidium bromide for the unfolding of bands (18S and 28S) under ultraviolet light. The RNA samples were treated with DNAse and then the cDNAs synthesis was processed using SuperScript from 2 μg of total RNA in the presence of random primers and oligo dT incubating at 42 °C for 50 min reverse transcription subsequently inactivating the enzyme by incubating at 70 °C for 15 min. The programming of RT-PCR experiments was followed: 1 cycle initial denaturation of 10 min at 95 °C, 40 cycles of amplification (30 sec denaturation at 95 °C and 1 min annealing and extension at 60 °C). Table 2 shows the sequence of the primers that were used.

Table 2. Sequence of primers used in the analysis of mRNA expression by RT-PCR

Primer	Forward	Reverse	GenBank NCBI Reference Sequence
HPRT	5'-AAG CTT GCT GGT GAA AAG GA-3'	5'-TGA TTC AAA TCC CTG AAG TGC-3'	NM_012583.2
COX-1	5'-CCT TCT CCA ACG TGA GCT ACT A-3'	5'-TCC TTC TCT CCT GTG AAC TCC T-3'	NM_017043.4
COX-2	5'-AGA CAG ATC ATA AGC GAG GAC C-3'	5'-CAC TTG CAT TGA TGG TGG CTG T-3'	NM_017232.3
iNOS	5'-ACA ACA GGA ACC TAC CAG CTC A-3'	5'-GAT GTT GTA GCG CTG TGT GTC A-3'	NM_012611.3
eNOS	5'-GGA GAA GAT GCC AAG GCT GCT G-3'	5'-CTT CCA GTG TCC AGA CGC ACC A-3'	NM_021838.2

Determination of PGE_2. The measurement of PGE_2 was determined using a commercial kit PGE_2 EIA — Monoclonal following the manufacturer's instructions in the samples of tumor tissue. Data were expressed in ng/g tissue.

Lipid peroxidation assay by the TBARS method. Samples of the solid tumor mass were weighed and homogenized in potassium phosphate buffer pH = 7.4 (5 ml buffer per 1 g tissue ratio) and protein quantification was quantified by the method of Bradford (1976) using a commercial kit. Two hundred microliters of homogenate were mixed with 400 μl of a solution containing: 15% trichloroacetic acid, 0.37% thiobarbituric acid and 00:25 hydrochloric. Then samples were maintained for 45 min at 90 °C and centrifuged for 15 min at 2000 g. The absorbance of a 200 μl of the supernatant was measured from 535 nm to 570 nm and corrected in an ELISA Reader (Spectramax plus 384, USA). The data were expressed in nmol of aldehyde/mg protein.

Myeloperoxidase (MPO) activity assay. Tissue samples from the solid tumor mass were homogenised

in a corresponding volume of 10× HTAB buffer. The tubes were heated for 2 h in an oven at 60 °C for inactivation of endogenous catalase activity and centrifuged at 12000 g for 2 min. Ten microliters of the supernatant were pipetted into 96 well microplate with 200 microliters of a solution of potassium phosphate buffer (pH = 6.0) containing 0,164 mg/ml o-dianisidine dihydrochloride and 0.0005% peroxide hydrogen, in duplicate. The MPO activity was measured at 460 nm in a microplate reader (Espectra Max Plus 384, USA) for 10 min and then was calculated from the maximum velocity reaction (Vmax) by seconds using a data acquisition program SOFTmax Pro Version 3.1.2 (Molecular Devices Corp., USA) spectrophotometer Espectra Max plus 384. The results were expressed in Units (U) of MPO/weight of solid tumor mass, and one unit of MPO is defined as the amount in μmol of H_2O_2 degraded per min.

Survival analysis. Survival data were analyzed using the Kaplan — Meier method. To compare the survival curves between the different groups the Log-Rank (Mantel Cox), Log-Rank for Trend and Gehan-Breslow-Wilcoxon tests were used. The median measures for the time variable (days) were calculated by interpolation using the estimates of survival.

Statistical analysis. One-way ANOVA followed by Turkey — Kramer multiple comparison test was performed. A p value less than 0.05 were considered the statistically significant difference. A Software Program GraphPad Prism Version 5.0 (Graph Pad Software Inc., USA) was utilized for all analyses.

RESULTS

The data of proinflammatory interleukins (IL-1β, IL-6, IL-10, TNF-α) levels after treatment protocol with different MB concentrations on Walker 256 carcinosarcoma (W256) solid tumor are illustrated in Fig. 1. No statistically significant difference was found in the IL-1β levels for different MB treated groups compared with the control group. Regarding IL-6, IL-10 and TNF-α levels we observed highly significant statistically increase of this indices only in the group treated with 0.1% MB compared to the different MB treated groups and the control group. Fig. 2 represents proinflammatory interleukins levels after a treatment association 0.1% MB + laser at 660 nm with different radiation dose (1 J/cm², 3 J/cm², 6 J/cm²) on W256 solid tumor. A statistically significant increase in levels of IL-1β, IL-6, IL-10, and TNF-α was found in the 0.1% MB + 1 J/cm² treated group compared to the control group and groups treated with 0.1% MB + 3 J/cm² and 0.1% MB + 6 J/cm², respectively.

The results of mRNA expression of COX-1, COX-2, iNOS, and eNOS after treatment protocol with different MB concentrations on W256 solid tumor are shown in Fig. 3. No statistically significant difference was found in the mRNA expression of COX-1 for different MB treated groups compared to control. Comparative analysis the mRNA expression of COX-2, iNOS and eNOS for different MB treated groups we found

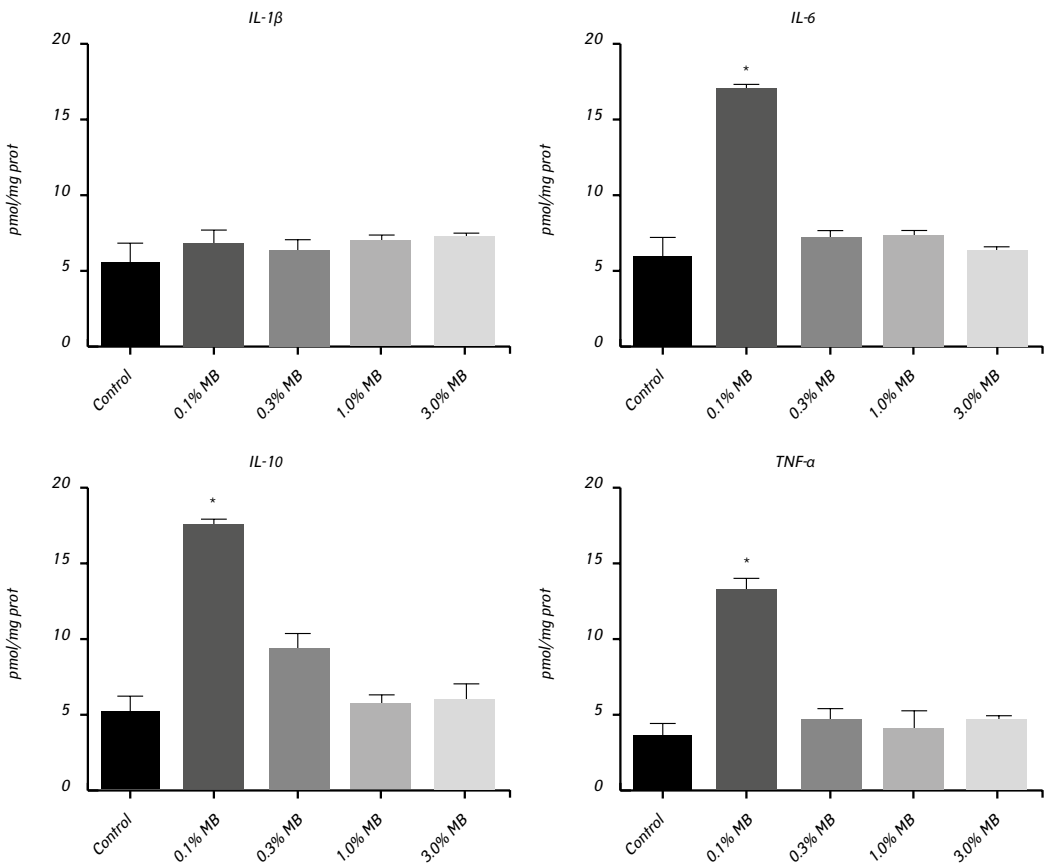

Fig. 1. Interleukins levels in W256 tissue after treatment with different MB concentrations. The data represent the mean ± SEM, n = 8, $p < 0.05$ compared to the control group (*$p < 0.001$ 0.1% MB *vs* control, *vs* 0.3% MB, *vs* 1.0% MB, *vs* 3.0% MB)

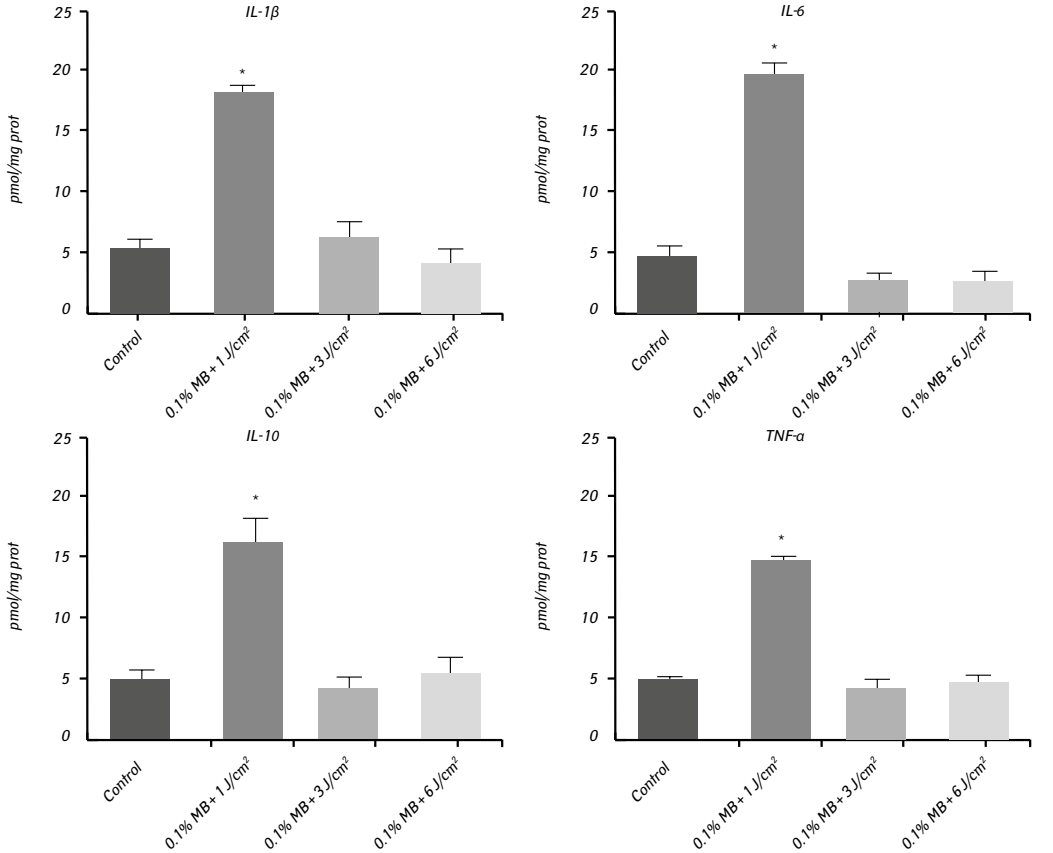

Fig. 2. Interleukins levels in W256 tissue after treatment with a combination of 1% MB and laser at 660 nm with different radiation dose (1 J/cm², 3 J/cm², 6 J/cm²). The data represent the mean ± SEM, n = 8, $p < 0.05$ compared to the control group (*$p < 0.001$ 0.1% MB + 1 J/cm² *vs* control, *vs* 0.1% MB + 3 J/cm², *vs* 0.1% MB + 6 J/cm²)

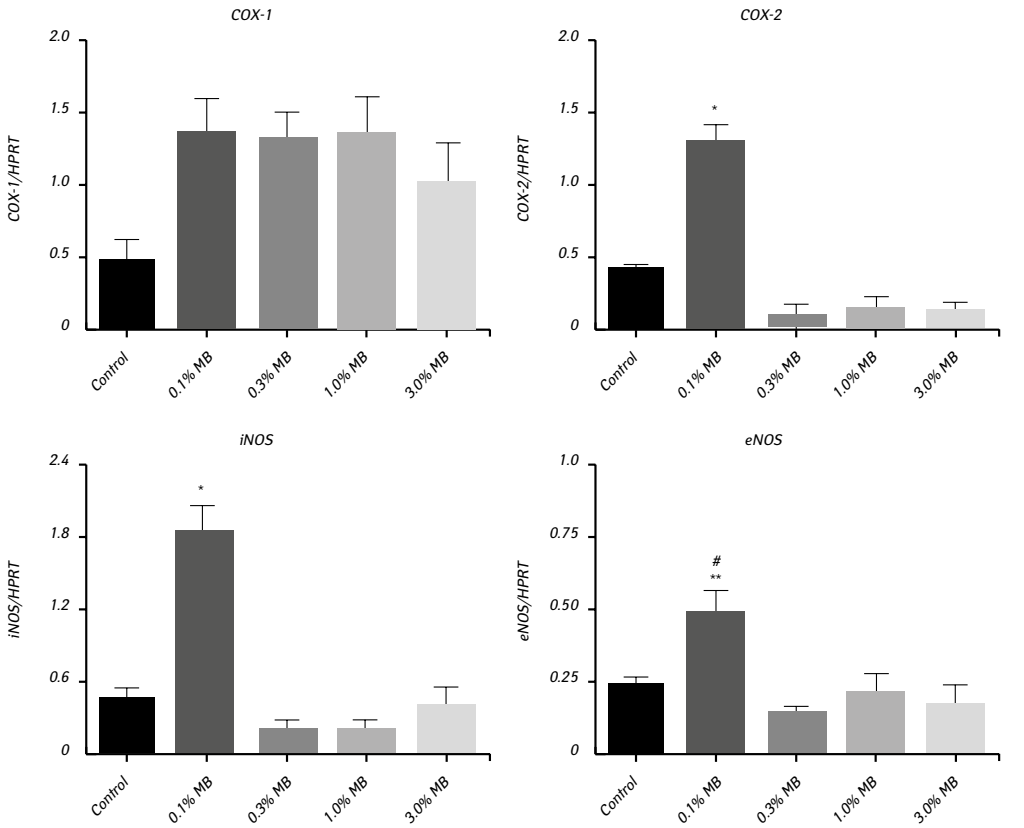

Fig. 3. The mRNA expression of COX-1, COX-2, iNOS, and eNOS in W256 tissue after treatment with different MB concentrations. The data represent the mean ± SEM, n = 8, $p < 0.05$ compared to the control group (COX-2: *$p < 0.001$ 0.1% MB *vs* control, *vs* 0.3% MB, *vs* 1.0% MB, *vs* 3.0% MB; iNOS: *$p < 0.001$ 0.1% MB *vs* control, *vs* 0.3% MB, *vs* 1.0% MB, *vs* 3.0% MB; eNOS: #$p < 0.5$ 0.1% MB *vs* control, **$p < 0.01$ 0.1% MB *vs* 0.3% MB, *vs* 1.0% MB, *vs* 3.0% MB)

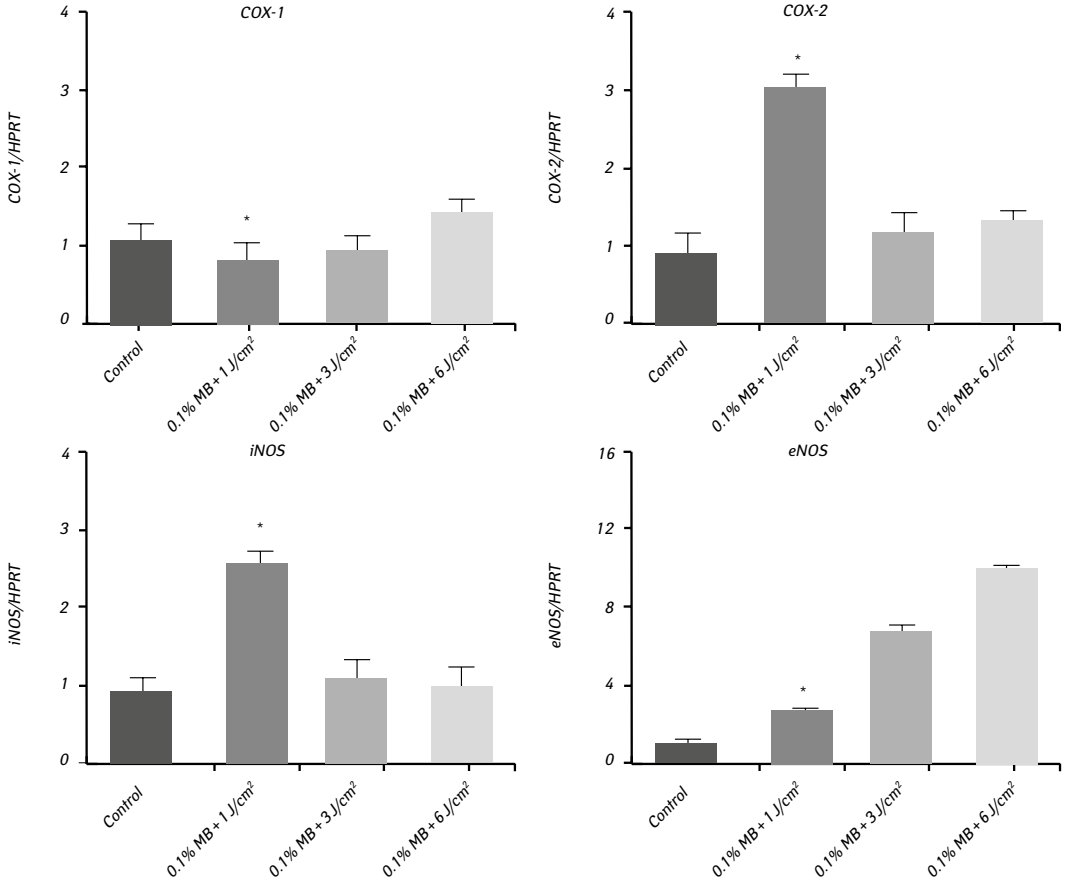

Fig. 4. The mRNA expression of COX-1, COX-2, iNOS, and eNOS in W256 tissue after treatment with a combination of 1% MB and laser at 660 nm with different radiation dose (1 J/cm², 3 J/cm², 6 J/cm²). The data represent the mean ± SEM, n = 8, $p < 0.05$ compared to the control group (*$p < 0.001$ 0.1% MB + 1 J/cm² *vs* control, *vs* 0.1% MB + 3 J/cm², *vs* 0.1% MB + 6 J/cm²)

a statistically significant increase of these indicators only in 0.1% MB treated group compared to control. Fig. 4 shows the mRNA expression of COX-1, COX-2, iNOS and eNOS on W256 solid tumor after its treatment with 0.1% MB and laser at 660 nm with different energy densities. No statistically significant difference was found comparing the mRNA expression of COX-1 in experimental and control groups. However, the expressions of mRNAs of COX-2 and iNOS were higher with a statistically significant difference in the group 0.1% MB + 1 J/cm² compared to other experimental groups or control. Regarding the expression of mRNA for eNOS, we observed a statistically significant reduction in the group 0.1% MB + 1 J/cm² compared to 0.1% MB + 3 J/cm² and 0.1% MB + 6 J/cm² groups, however, a small statistically significant increase was found compared to the control group.

Table 3 shows the data of PGE_2 and TBARS levels, and MPO activity in W256 tumor tissue following treatment protocol with an association of 0.1% MB + laser at 660 nm with different radiation dose. Statistically significant increase of PGE_2 and TBARS levels and MPO activity ($p < 0.001$) was observed in 0.1% MB + 1 J/cm² treated group compared to other experimental and control groups.

Survival curves calculated by Kaplan — Meier for different MB treated and control groups are shown in Fig. 5. We can verify a greater probability of survival in the 0.1% MB and 0.3% MB treated groups compared to the control. Regarding 1.0% MB and 3.0% MB treated groups shows the same probability of survival as the control group. Fig. 6 represents the results of survival curves estimation by Kaplan — Meier method for different 0.1% MB + laser treated and control groups. We found a greater probability of survival in 0.1% MB + 1 J/cm² group compared to the control.

DISCUSSION

PDT, a FDA-approved anticancer therapy has been used for clinical treatment several late-stage cancers in the United States, European Union, Canada,

Table 3. Levels of PGE_2, TBARS and MPO activity in W256 tissue after treatment with a combination of 1% MB and laser at 660 nm with different radiation dose (1 J/cm², 3 J/cm², 6 J/cm²)

Treatment groups (n = 8)	Dose, mg/ml	Energy dose, J/cm²	Total energy dose (4 points), J/cm²	PGE_2, pg/mg prot	TBARS, nmol/g	MPO, UMPO/g
Control	–	–	–	243.5 ± 0.7	1.43 ± 0.14	0.8 ± 0.4
MB 0.1% + laser 1 J/cm²	1	35.7	142.8	804.1 ± 0.55*	2.75 ± 0.26*	537.6 ± 0.6*
MB 0.1% + laser 3 J/cm²	1	107.14	428.56	143.3 ± 0.65	1.32 ± 0.11	4.3 ± 0.6
MB 0.1% + laser 6 J/cm²	1	214.28	857.12	214.8 ± 0.59	1.32 ± 0.13	2.8 ± 0.7

Note: The data represent the mean ± SEM, $p < 0.05$ compared to the control group (*$p < 0.001$ 0.1% MB + 1 J/cm² *vs* control, *vs* 0.1% MB + 3 J/cm², *vs* 0.1% MB + 6 J/cm²). Ø spot size area = 0.028 cm².

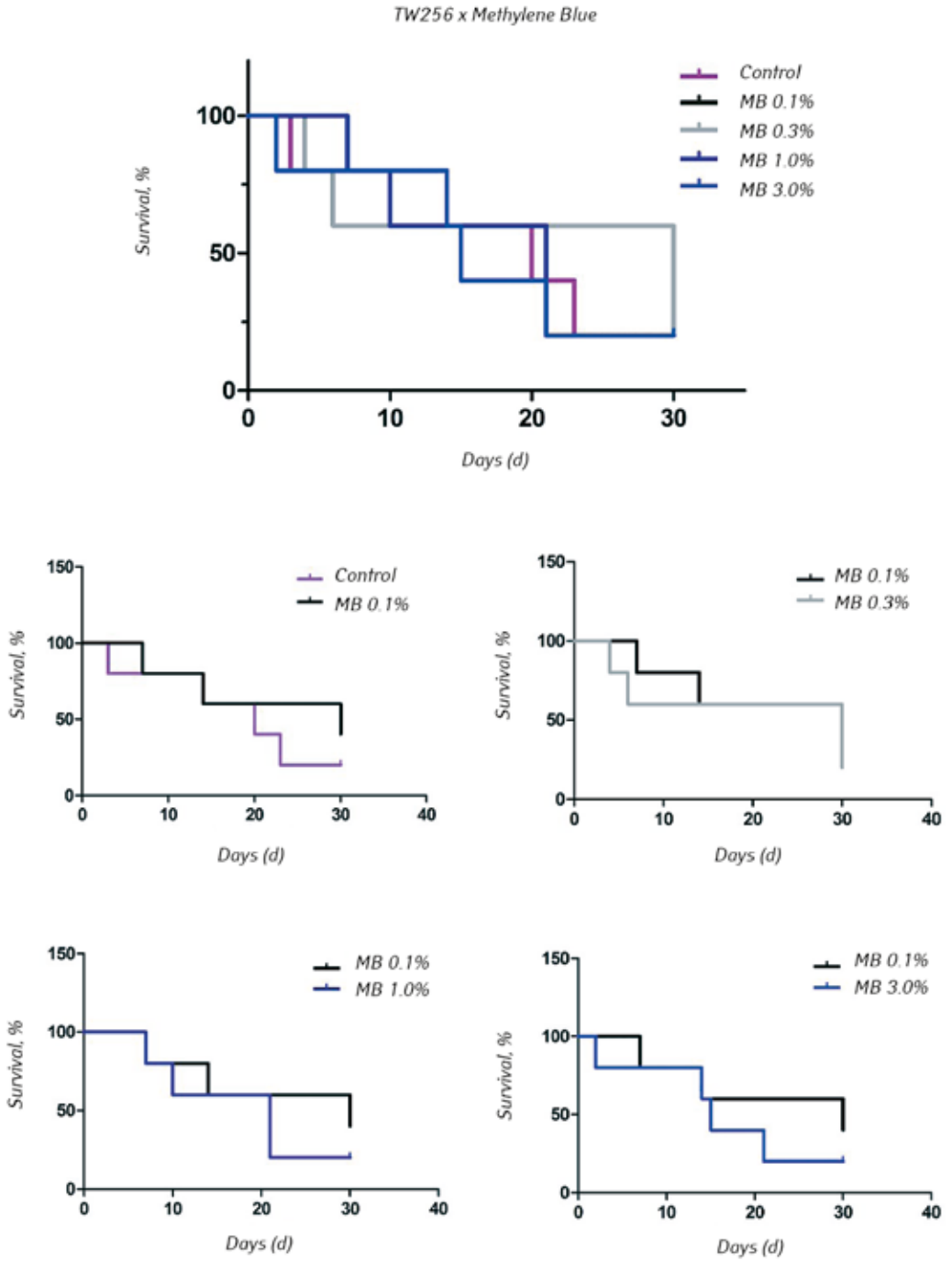

Test	Chi square	df	*p* value
Log-rank	0.9035	4	0.9241
Lograng for trend	0.1744	1	0.6762

Fig. 5. Estimation of survival by Kaplan — Meier curves for groups treated with different MB concentrations and control group

Russia, and Japan. MB is a widely studied agent currently under investigation for its properties relating to PDT. Recent studies have demonstrated that MB exhibits profound phototoxicity affecting a variety of cancer cells. However, the mechanistic explanation for MB-mediated PDT is not yet fully elucidated.

In this work, we evaluated the inflammatory aspects of MB-mediated PDT in an experimental rat model of W256. Intratumorally applied of MB in the 0.1% concentration caused an increase of interleukins (IL-6, IL-10, TNF-α) levels and mRNA expression of COX-1, COX-2, iNOS and eNOS in tumor tissue. Thus, we can indicate "dark toxicity effects" suggesting that the 0.1% concentration of MB as the best dose to be used in PDT. Treatment with 0.1% MB + 1 J/cm^2 promoted increase interleukins levels (IL-1β, IL-6, IL-10, and TNF-α), PGE_2, mRNA expression of COX-1, COX-2, iNOS, lipid peroxidation levels and MPO activity in tumor tissue.

Currently, it has been fully understood the fundamental role of ROS in the process of initiation and progression of cancer. The mutagenic action induced by ROS is a critical factor in carcinogenesis initiation. Therefore, signaling mutagenicity mediated

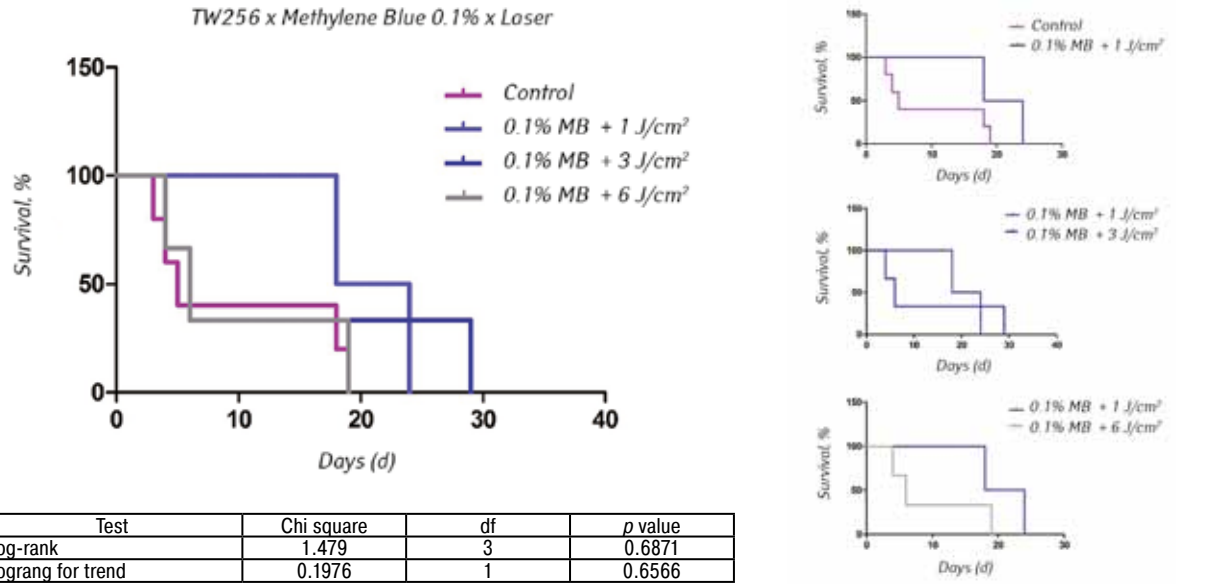

Test	Chi square	df	*p* value
Log-rank	1.479	3	0.6871
Lograng for trend	0.1976	1	0.6566

Fig. 6. Estimation of Kaplan — Meier curves for different groups treated with a combination of 0.1% MB + laser at 660 nm with different radiation dose and control group

by ROS, the control of apoptotic pathways and survival are important factors that contribute to malignant transformation and progression [29, 30]. Moreover, constitutively elevated levels of cellular oxidative stress and dependency on ROS signaling may exhibit a redox vulnerability of malignancy that may become targeted by chemotherapeutic intervention using redox modulators, anti- and prooxidant agents have been shown to exert anticancer activity [29]. In fact, redox agents such as phenothiazines redox cycles inclusive MB have been used in diverse applications as biological redox indicators. However, it has demonstrated potential anticancer therapy as redox chemotherapeutic that can promote selective cytotoxicity in cancer cells. Nevertheless, its mechanism of action remains under investigation [24, 32–34]. Recent research suggests that MB induce selective cancer cell apoptosis by NAD(P)H: quinine oxidoreductase (NQO1)-dependent bioreductive generation of cellular oxidative stress [21, 31]. Once MB actively links to mitochondria and goes into the matrix in a way induced through the mitochondrial proton potential [24, 35, 36]. MB accumulation in the mitochondria causes the MB reduction to the leuco-MB and consequently in the oxidation of NAD(P)H mitochondrial followed by ROS generation and finally cytotoxicity [35].

The cytotoxicity of MB was evaluated in this work by proinflammatory interleukins levels and mRNA expression of COX-1, COX-2, iNOS and eNOS in the solid tumor mass. After using of 0.1% MB we found an increase of IL-6, IL-10 and TNF-α levels, mRNA expression of COX-2, iNOS and eNOS. This is due to the generation of oxidative stress induced by MB since it is present inside the mitochondria and is converted to leuco-MB leading to the formation of ROS. Therefore, this oxidative stress triggers an increase in the generation of antigens that stimulate the expression of these proinflammatory mediators via NF-kB and activator protein 1 (AP-1) promoting inflammation and cellular damage. The gene expression of iNOS and the subsequent translation of the mRNA is controlled by a broad number of proinflammatory mediators, particularly IL-1β and TNF-α [45], which can be interpreted as cytotoxic effects on tumor cells. However, eNOS is one of the constitutive isoforms of nitric oxide (NO) synthase involved in the angiogenesis process. We observed the increase of eNOS and suggest that tumor tends to combat the cytotoxic effects by promoting the formation of new vessels. The treatment of W256 with high concentrations of MB does not cause to the increase of proinflammatory interleukins levels as well as mRNA expression of COX-1, COX-2, iNOS, and eNOS and we suggest that at higher concentrations of MB may occur the formation MB dimer and thereby losing their effectiveness.

Despite the fact that the exact mechanisms of action of PDT are not firmly established, it is accepted that in PDT implies the interaction of oxygen, photosensitization, and light. Once PS is excited and activated through light, interacts with molecular oxygen that is converted into yield reactive singlet oxygen ($^1O_2$), the suggest mediator of photodynamic cytotoxicity (type 2 photo-oxidation). Then $^1O_2$ interacts with biomolecules producing oxy-cytotoxic products [37, 38]. Research has shown that during the process of PDT, excitation of PS with light yields reactive short-lived $^1O_2$ and ROS, which causes an immediate oxidative alteration of biomolecules, especially proteins and lipids. The main PDT-induced alteration is protein oxidation, which thereafter induces to protein fragmentation, cross-linking, carbonylation, aggregation, adduct formation, unfolding, and conformational changes [39, 40]. As most of PSs have the affinity to membranes, lipids are the primary targets of ROS. The photo-oxidative alteration of membrane lipids leads to the generation of intermediate lipid hydroperoxides, which

modify circulating molecules and ultimately amplifies the damage begun by ROS within cells. These events contribute to lipid peroxidation, photooxidation of guanine DNA and damage to membranes, cytoskeleton, and other sites and ultimately cell death and tissue destruction [39, 41].

In this work, we evaluated the cytotoxic effects of MB, mediated by PDT, with lipid peroxidation assay — TBARS method. We can see that treatment of W256 with 0.1% MB + 1 J/cm^2 promote photodynamic action and leading to the formation of singlet oxygen and ROS thereby producing oxidative stress and cell damage that was evidenced by the high levels of lipid peroxidation produced. Because of the non-occurrence of photodynamic effect when we use higher doses of laser energy is given by the possibility of important structural alterations have occurred in the MB molecule leading to their inactivation and thus lose its effectiveness.

It's broadly understood that PDT promotes oxidative stress and triggers a wide range of signaling pathways by Toll-like receptors that generates protective responses. This comprises expression of heat shock proteins and transcription factors such as NF-κB and AP-1. Then NF-κB and AP-1 can urges the expression of immunoregulatory and proinflammatory proteins particularly interleukins (IL-1α, IL-1β, IL-2, IL-6, IL-8, IL-10), TNF-α, chemokines (inflammatory protein IP-10, keratinocytes-derived chemokines KC, macrophage inflammatory proteins MIP-1α and MIP-β, MIP-2, RANTES), interferons (IFN-α and IFN-β), COX-2, eicosanoids like leukotrienes, thromboxane and prostaglandins, even as histamine, NO, molecular adhesion factors and components of the complement system (C3 and C5) [5, 6, 16, 42, 43]. These mediators once released are responsible for complement system activation, maturation of DCs, recruitment of macrophages and natural killer cells, and neutrophil infiltration within the tumor site [5, 6, 44]. Recent research indicates that high neutrophil in the tumor tissue mediated by PDT acts a crucial role in the maturation of DCs, macrophage activation and activation of natural killer cells. Thus this promoting the recognition of antigens such as the damage-associated molecular patterns necessary for activation of cytotoxic $CD8^+$/$CD4^+$ lymphocytes. Therefore, creating an effective innate and adaptive immune response in the long term control of tumor progression [6, 16, 18, 37, 43, 44].

The expression of proinflammatory mediators was investigated in the W256 tumor tissue. In the group with 0.1% MB + 1 J/cm^2 treatment combination we observed an increase of all inflammatory interleukins levels, PGE_2, and mRNA expression of COX-2. These changes are owing to the generation of oxidative stress induced by photosensitizing of MB during PDT. Thus this oxidative stress provoked by cellular damage triggers increased expression of antigens prompts to the generation of these proinflammatory mediators via NF-kB and AP-1 activation.

The involvement of NO in the initiation and progression of cancer has aroused great concern. Research has focused on how NO produced in cancer cells or by cancer cells themselves can influence both positively and negatively on the anticancer efficacy of PDT. NO synthases are part of a group of enzymes isoforms that catalyze the generation of NO from the amino acid L-arginine, and iNOS is the main enzyme that produces large amounts of NO as a mechanism of defense. Therefore, NO derived from iNOS plays a key role in cell signaling under various physiological (blood pressure regulation, wound repair and host defense mechanisms) and pathological (inflammation, infection, neoplastic diseases, liver cirrhosis, diabetes) conditions. In addition, iNOS is frequently linked with malignancy. However, macrophage-derived NO has demonstrated a potentially cytotoxic/cytostatic effect on tumor cells. Expression of the iNOS gene and the subsequent translation of the mRNA are regulated through proinflammatory markers. The most prominent cytokines, involved in the stimulation of iNOS, are TNF-α, IL-1, and IFN-γ [45]. We also observed an increase of iNOS gene expression that confirms with a raise of IL-1 and TNF-α levels suggesting tumoricidal activity in the group with 0.1% MB + 1 J/cm^2 treatment combination. Interestingly, we noted a significant reduction in the expression of the eNOS gene, which is one of the constitutive isoforms of NO synthase that associated in angiogenesis, affecting the formation of new blood vessels in the supply of oxygen and nutrients to tumor cells, thus contributing to the reduction of the tumor.

These findings lead to suggest the presence of cellular damage and inflammation in tumor tissue. There is evidence of increased expression of antigens derived from tumor cells induces the maturation of DCs, recruitment of macrophages, natural killer cells, promoting neutrophil infiltration within the tumor site and thus stimulate an immune response. The generation of an antitumor immune response as well as memory response of $CD4^+$- and $CD8^+$-T cells is largely dependent on the high neutrophil infiltration levels that can be measured by MPO activity [5]. MPO activity levels also increased in W256 tissue after 0.1% MB + 1 J/cm^2 treatment combination suggesting evidence an immune response against the tumor.

The results of the survival analysis corroborate previous findings, demonstrating that the groups treated with 0.1% MB and 0.1% MB + 1 J/cm^2 had median survival time values of 30 days, which presented a higher probability of survival.

According to our findings, we can conclude that treatment of W256 with 0.1% MB + 1 J/cm^2 was able to generate cytotoxic effects in the tumor by increasing ROS, which consequently raises the expression of inflammatory mediators, promoting inflammation triggering damage and death of cancer cells. There is evidence of a tumoricidal activity of neutrophils in the solid tumor mass suggesting an antitumor immune response and thus promoting the long-term control of tumor growth and progression.

COMPLIANCE WITH ETHICAL STANDARDS

Funding: This study was funded by Fundação de Amparo à Pesquisa do Estado de São Paulo (FAPESP): 07/59124-0.

Conflict of Interest: Only E.C.P. Leal-Junior has conflict of interest. The other authors do not have.

Statement on the welfare of animals: All procedures performed in studies involving animals were in approved with The Animal Experimentation Ethics Committee (CEEA) of the Institute of Biomedical Sciences, University of São Paulo, Protocol Number 67 fl 73 L2-5351 or practice at which the studies were conducted.

ACKNOWLEDGMENTS

Fundação de Amparo à Pesquisa do Estado de São Paulo (FAPESP): 07/59124-0.

REFERENCES

1. **Anand S, Ortel BJ, Pereira SP, *et al.*** Biomodulatory approaches to photodynamic therapy for solid tumors. Cancer Lett 2012; **326**: 8–16.

2. **Hasan T, Ortel B, Solban N, Pogue B.** Photodynamic therapy of cancer. Cancer Medicine, 7th ed. Hamilton, Ontario: BC Decker Inc, 2006: 537–48.

3. **Celli JP, Spring BQ, Rizvi I, *et al.*** Imaging and photodynamic therapy: mechanisms, monitoring, and optimization. Chem Rev 2010; **110**: 2795–838.

4. **Buytaert E, Dewaele M, Agostinis P.** Molecular effectors of multiple cell death pathways initiated by photodynamic therapy. Biochim Biophys Acta 2007; **1776**: 86–107.

5. **Garg AD, Nowis D, Golab J, Agostinis P.** Photodynamic therapy: illuminating the road from cell death towards anti-tumour immunity. Apoptosis 2010; **15**: 1050–71.

6. **Pizova K, Tomankova K, Daskova A, *et al.*** Photodynamic therapy for enhancing antitumour immunity. Biomed Pap Med Fac Univ Palacky Olomouc Czech Repub 2012; **156**: 93–102.

7. **Robertson CA, Evans DH, Abrahamse H.** Photodynamic therapy (PDT): a short review on cellular mechanisms and cancer research applications for PDT. J Photochem Photobiol B 2009; **96**: 1–8.

8. **Agostinis P, Berg K, Cengel KA, *et al.*** Photodynamic therapy of cancer: an update. CA Cancer J Clin 2011; **61**: 250–81.

9. **O'Connor AE, Gallagher WM, Byrne AT.** Porphyrin and nonporphyrin photosensitizers in oncology: preclinical and clinical advances in photodynamic therapy. Photochem Photobiol 2009; **85**: 1053–74.

10. **García-Díaz M, Kawakubo M, Mroz P, *et al.*** Cellular and vascular effects of the photodynamic agent temocene are modulated by the delivery vehicle. J Control Release 2012; **162**: 355–63.

11. **Krammer B.** Vascular effects of photodynamic therapy. Anticancer Res 2001; **21**: 4271–7.

12. **Preise D, Scherz A, Salomon Y.** Antitumor immunity promoted by vascular occluding therapy: lessons from vascular-targeted photodynamic therapy (VTP). Photochem Photobiol Sci 2011; **10**: 681–8.

13. **St Denis TG, Aziz K, Waheed AA, *et al.*** Combination approaches to potentiate immune response after photodynamic therapy for cancer. Photochem Photobiol Sci 2011; **10**: 792–801.

14. **Korbelik M.** Cancer vaccines generated by photodynamic therapy. Photochem Photobiol Sci 2011; **10**: 664–9.

15. **Bhuvaneswari R, Gan YY, Soo KC, Olivo M.** The effect of photodynamic therapy on tumor angiogenesis. Cell Mol Life Sci 2009; **66**: 2275–83.

16. **Kwitniewski M, Juzeniene A, Glosnicka R, Moan J.** Immunotherapy: a way to improve the therapeutic outcome of photodynamic therapy? Photochem Photobiol Sci 2008; **7**: 1011–7.

17. **Kousis PC, Henderson BW, Maier PG, Gollnick SO.** Photodynamic therapy enhancement of antitumor immunity is regulated by neutrophils. Cancer Res 2007; **67**: 10501–10.

18. **Yang D, de la Rosa G, Tewary P, Oppenheim JJ.** Alarmins link neutrophils and dendritic cells. Trends Immunol 2009; **30**: 531–7.

19. **Tracy EC, Bowman MJ, Henderson BW, Baumann H.** Interleukin-1α is the major alarmin of lung epithelial cells released during photodynamic therapy to induce inflammatory mediators in fibroblasts. Br J Cancer 2012; **107**: 1534–46.

20. **Dobson J, de Queiroz GF, Golding JP.** Photodynamic therapy and diagnosis: principles and comparative aspects. Vet J 2018; **233**: 8–18.

21. **Ginimuge PR, Jyothi SD.** Methylene blue: revisited. J Anaesthesiol Clin Pharmacol 2010; **26**: 517–20.

22. **Jena S, Chainy GB.** Effect of methylene blue on oxidative stress and antioxidant defence parameters of rat hepatic and renal tissues. Indian J Physiol Pharmacol 2008; **52**: 293–6.

23. **Schirmer RH, Adler H, Pickhardt M, Mandelkow E.** Lest we forget you — methylene blue... Neurobiol Aging 2011; **32**: 2325.e7–16.

24. **Tardivo JP, Del Giglio A, de Oliveira CS, *et al.*** Methylene blue in photodynamic therapy: From basic mechanisms to clinical applications. Photodiagnosis Photodyn Ther 2005; **2**: 175–91.

25. **Auerbach SS, Bristol DW, Peckham JC, *et al.*** Toxicity and carcinogenicity studies of methylene blue. Food Chem Toxicol 2010; **48**: 169–77.

26. **Lu Y, Jiao R, Chen X, *et al.*** Methylene blue-mediated photodynamic therapy induces mitochondria-dependent apoptosis in HeLa cell. J Cell Biochem 2008; **105**: 1451–60.

27. **Peloi LS, Soares RR, Biondo CE, *et al.*** Photodynamic effect of light-emitting diode light on cell growth inhibition induced by methylene blue. J Biosci 2008; **33**: 231–7.

28. **Chen Y, Zheng W, Li Y, *et al.*** Apoptosis induced by methylene-blue-mediated photodynamic therapy in melanomas and the involvement of mitochondrial dysfunction revealed by proteomics. Cancer Sci 2008; **99**: 2019–27.

29. **Wondrak GT.** NQO1-activated phenothiazinium redox cyclers for the targeted bioreductive induction of cancer cell apoptosis. Free Radic Biol Med 2007; **43**: 178–90.

30. **Wu WS.** The signaling mechanism of ROS in tumor progression. Cancer Metastasis Rev 2006; **25**: 695–705.

31. **Cen D, Brayton D, Shahandeh B, *et al.*** Disulfiram facilitates intracellular Cu uptake and induces apoptosis in human melanoma cells. J Med Chem 2004; **47**: 6914–20.

32. **Miller RA, Woodburn KW, Fan Q, *et al.*** Motexafin gadolinium: a redox active drug that enhances the efficacy of bleomycin and doxorubicin. Clin Cancer Res 2001; **7**: 3215–21.

33. **Renschler MF.** The emerging role of reactive oxygen species in cancer therapy. Eur J Cancer 2004; **40**: 1934–40.

34. **Fry FH, Holme AL, Giles NM, *et al.*** Multifunctional redox catalysts as selective enhancers of oxidative stress. Org Biomol Chem 2005; **3**: 2579–87.

35. **Rugolo M, Lenaz G.** Monitoring of the mitochondrial and plasma membrane potentials in human fibroblasts by tetraphenylphosphonium ion distribution. J Bioenerg Biomembr 1987; **19**: 705–18.

36. **Gabrielli D, Belisle E, Severino D, *et al.*** Binding, aggregation and photochemical properties of methylene blue in mitochondrial suspensions. Photochem Photobiol 2004; **79**: 227–32.

37. **His RA, Rosenthal DI, Glatstein E.** Photodynamic therapy in the treatment of cancer: current state of the art. Drugs 1999; **57**: 725–34.

38. **Moan J, Berg K.** The photodegradation of porphyrins in cells can be used to estimate the lifetime of singlet oxygen. Photochem Photobiol 1991; **53**: 549–53.

39. **Firczuk M, Nowis D, Gołąb J.** PDT-induced inflammatory and host responses. Photochem Photobiol Sci 2011; **10**: 653–63.

40. **Buytaert E, Dewaele M, Agostinis P.** Molecular effectors of multiple cell death pathways initiated by photodynamic therapy. Biochim Biophys Acta 2007; **1776**: 86–107.

41. **Girotti AW.** Photosensitized oxidation of membrane lipids: reaction pathways, cytotoxic effects, and cytoprotective mechanisms. J Photochem Photobiol B 2001; **63**: 103–13.

42. **Matroule JY, Volanti C, Piette J.** NF-kappaB in photodynamic therapy: discrepancies of a master regulator. Photochem Photobiol 2006; **82**: 1241–6.

43. **Panzarini E, Inguscio V, Dini L.** Immunogenic cell death: can it be exploited in PhotoDynamic Therapy for cancer? Biomed Res Int 2013; **2013**: 482160.

44. **Brodin NP, Guha C, Tomé WA.** Photodynamic therapy and its role in combined modality anticancer treatment. Technol Cancer Res Treat 2015; **14**: 355–68.

45. **Lechner M, Lirk P, Rieder J.** Inducible nitric oxide synthase (iNOS) in tumor biology: the two sides of the same coin. Semin Cancer Biol 2005; **15**: 277–89.